Journal of Molecular Liquids 346 (2022) 118292

Contents lists available at ScienceDirect

Journal of Molecular Liquids

journal homepage: www.elsevier.com/locate/molliq

Recovery of dialkylimidazolium-based ionic liquids from their mixtures with acetone or water by flash distillation

Nuria Caeiro [1], Marta K. Wojtczuk [2], Héctor Rodríguez, Eva Rodil *, Ana Soto

CRETUS, Department of Chemical Engineering, Universidade de Santiago de Compostela, E-15782 Santiago de Compostela, Spain

ARTICLE INFO

Article history:
Received 6 September 2021
Revised 30 November 2021
Accepted 6 December 2021
Available online 9 December 2021

Keywords:
Ionic liquid
Solvent recovery
Vapour-liquid equilibrium
Process simulation
Flash distillation

ABSTRACT

In a number of applications for which novel processes based on ionic liquids have been proposed, the recovery of the ionic liquid from its mixture with a molecular solvent is a step of critical importance for the viability of the process. In this work, feasibility and conditions for such recovery by simple flash vapourisation have been explored for the particular case of three dialkylimidazolium-based ionic liquids (namely 1-ethyl-3-methylimidazolium thiocyanate ([C_2mim][SCN]), 1-ethyl-3-methylimidazolium acetate ([C_2mim][OAc]), and 1-butyl-3-methylimidazolium acetate ([C_4mim][OAc])) and either acetone or water as representative molecular solvents of industrial relevance. The isobaric vapour-liquid equilibria of the binary systems acetone + ([C_2mim][SCN] or [C_4mim][OAc]) and water + ([C_2mim][OAc] or [C_4mim][OAc]) have been determined at three different pressures (101.32, 50.00, and 30.00 or 25.00 kPa), and the data have been suitably correlated by means of the NRTL thermodynamic model. These correlations have been used in the software Aspen Plus for the development of reliable simulations of a flash unit to perform the desired separations. The results indicate the difficulty in getting the ionic liquids recovered with high purity, even if operating the flash at a pressure as low as 5 kPa and at temperatures close to the range where the thermal stability of the ionic liquids starts to get compromised.
© 2021 The Authors. Published by Elsevier B.V. This is an open access article under the CC BY license (http://creativecommons.org/licenses/by/4.0/).

1. Introduction

One of the pillars for the development of chemical processes in industry with improved performance and sustainability credentials is the reduction of auxiliary substances as ubiquitous as organic solvents. Where not possible, an appealing option is their substitution by more benign solvents. In this vein, ionic liquids (ILs) [1,2] have been proposed over the last couple of decades as an alternative to conventional volatile organic solvents in a varied range of applications. Within the set of characteristics that ILs usually exhibit, the following can be cited to illustrate the potential attractiveness of their use as neoteric solvents: negligible vapour pressure (thus resulting in no direct contribution to atmospheric pollution and in a safer and healthier working environment), great solvation ability, and wide temperature range as stable liquids [1,3].

After its utilisation in a reaction or separation unit, the IL (like generally any other solvent) will end up mixed with other components in the outlet fluid stream of the unit. This is also the case when using an antisolvent strategy to precipitate non-volatile solutes out of an IL solution, which is an approach commonly adopted in the promising application of (pre)treatment and fractionation of lignocelluloses with ILs [4–6]. The efficient recovery of the IL for its recycling to the corresponding unit upstream is a key aspect to evaluate not only the technical but also the economic viability (as it can entail a significant energy penalty) of the proposed IL-based process [6–8]. Despite its critical character, limited attention has been paid to this aspect in the literature to date, possibly due in part to the frequent assumption that the recovery of the non-volatile IL from the volatile substances with which it is mixed is trivial by any vapourisation technique (for instance, evaporation or distillation). Although the enormous difference in volatility may certainly suggest the utilisation of a technique such as flash distillation, the difficulty in accomplishing the recovery of the IL must be assessed through knowledge of the thermodynamic phase behaviour of the intended system. Moreover, this information on the phase behaviour is crucial for a proper engineering design of the solvent recovery equipment.

In this work, an investigation has been made of the feasibility of recovery of specific ILs from their mixtures with water or with acetone, which represent two of the most widely used molecular solvents in process plants in the (bio)chemical industry. The selected ILs for the study were: 1-ethyl-3-methylimidazolium thiocyanate

* Corresponding author.
E-mail address: eva.rodil@usc.es (E. Rodil).
[1] Present address: Trivium Packaging, Carretera C-531, p.k. 13,8, 36616 Meis, Spain.
[2] Present address: OSIsoft Europe GmbH, Mainzer Landstraße 178-190, 60327 Frankfurt am Main, Germany.

https://doi.org/10.1016/j.molliq.2021.118292
0167-7322/© 2021 The Authors. Published by Elsevier B.V.
This is an open access article under the CC BY license (http://creativecommons.org/licenses/by/4.0/).

([C_2mim][SCN]), 1-ethyl-3-methylimidazolium acetate ([C_2mim][OAc]), and 1-butyl-3-methylimidazolium acetate ([C_4mim][OAc]). These are three ILs constituted by a 1-alkyl-3-methylimidazolium cation, corresponding to the most popular type of IL-forming cations, and an anion which is the conjugated base of a weak acid, and therefore will present a certain basicity (hydrogen bond acceptor ability). The latter is a characteristic of potential interest for attractive applications such as the pretreatment/fractionation of lignocellulosic biomass [4,9] or the capture of CO_2 [10]. The set of these three ILs allows, moreover, the analysis of two different IL structural features: the effect of the length of the alkyl substituent chain in the cation ([C_2mim][OAc] versus [C_4mim][OAc]) and the nature of the anion ([C_2mim][SCN] versus [C_2mim][OAc]). The approach followed has consisted on the experimental determination of rigorous vapour-liquid equilibrium data for the selected binary systems (supported by previous characterisation of specific physical properties), and subsequent utilisation of this phase equilibrium information for the reliable simulation of the IL recovery unit in an industrial context via a chemical process simulation software [11–13]. This simulation has enabled an easy exploration and identification of the optimal conditions of the IL recovery for each of the investigated systems, with particular attention being paid to the recovered IL purity and the energy requirements.

2. Materials and methods

2.1. Chemicals

General characteristics of the chemicals used in this work are presented in Table 1. Bidistilled water was used throughout this work. For reducing the water content of the hygroscopic ILs prior to their use (as this parameter is known to critically influence the performance of ILs [14]), they were dried under vacuum (absolute pressure lower than 1 Pa) at moderate temperature (ca. 333–343 K) for no less than 48 h. The dried ILs were analysed by ^{1}H and ^{13}C NMR spectroscopy, confirming the expected chemical structures and the absence of significant organic impurities. The corresponding spectra are shown in Figs. S1 to S6 in the Supplementary Material.

The final water content of the compounds to be used in the experimental work was measured in a Metrohm 899 coulometer by the Karl-Fischer titration method. The obtained values are reported in Table 2. Two physical properties of reference such as density and refractive index were measured (as described in Section 2.2 below) for all five compounds, and these values are also reported in Table 2 and compared to literature values [15–18].

2.2. Vapour-liquid equilibrium

Isobaric VLE data for the binary systems IL + (acetone or water) were obtained in a Fischer Labor und Verfahrenstechnik Labodest 602 distillation apparatus that recycles both liquid and vapour phases, equipped with a Fischer digital manometer and an ASL F250 Mk II precision thermometer operating with a wired PT100 PRT probe. Distillation was performed at absolute pressures of 30 kPa (or 25 kPa) and 50 kPa, assisted by a vacuum pump system, and at 101.32 kPa, precisely adjusted with the help of an external handmade constant-pressure system based on a side connection ending in a hollow rod partially immersed in an open glycerine column. In all cases, prior to the development of the equilibrium measurements, the air in the apparatus was displaced with inert argon (Praxair, 99.9%). For each overall composition charged in the still at a given pressure, the boiling temperature was recorded after equilibration, and samples of the liquid phase and the condensed vapour phase were taken by means of glass syringes coupled to stainless steel needles. For the compositional analysis of the phases in equilibrium, the densities of the samples from the liquid phase were measured and compared to a calibration curve. This calibration curve was built by finely correlating the excess molar volumes (using a Redlich-Kister polynomial – see Section 3.1) derived from the measurement of densities of samples of known composition (prepared by weight in a Mettler Toledo XPE205 analytical balance with a precision of 0.1 mg), covering the entire composition range. The densities of the samples from the vapour phase were only occasionally measured, to simply verify that the result matched that of pure acetone or pure water, as expected from the non-volatile nature of the ILs. All density measurements were carried out at atmospheric pressure in an Anton Paar DSA 48 vibrating U-tube density meter equipped with a built-in temperature control system (precise to within 0.1 K), and with automatic correction of the influence of the viscosity of the sample. Additionally, the samples were further characterised by measuring the speed of sound through them (performed simultaneously with the density measurements in the same apparatus) and their refractive indices. The latter were measured in an ATAGO RX-5000 refractometer coupled with a HetoTherm thermostat for temperature control. At least two measurements of each property were performed at 298.2 K and atmospheric pressure, checking repeatability within the respective uncertainties (0.0001 g/cm^3 for density, 1 m/s for speed of sound, and 0.00004 for refractive index), and the average values were recorded.

2.3. Process simulation

Simulations were performed with the commercial software Aspen Plus, version 10. In this version, the ILs investigated in this work do already appear in the compounds database, although a number of properties are missing. In order to define more completely these ILs, the following properties from the literature [19] were introduced: critical temperature, critical pressure, critical molar volume, critical compressibility factor, and theoretical normal boiling temperature. Moreover, vapour pressure and heat capacity correlation parameters from the literature [20–23] were also added in the definition of these ILs. All these parameters are presented in the Supplementary Material (Table S1). The NRTL thermodynamic model [24] was chosen to describe the non-ideal behaviour of the liquid phase, as this classical activity coefficient model has been found to provide a good correlation of vapour-liquid equilibrium behaviour in analogous binary systems [11].

Table 1
General characteristics of the chemicals used in this work.

Full name	Abbreviation	Chemical formula	Molar mass (g/mol)	CAS number	Source	Nominal purity
Acetone	–	C_3H_6O	58.08	67–64-1	Merck	99.5%
Water	–	H_2O	18.015	7732–18-5	bidistilled	–
1-ethyl-3-methylimidazolium acetate	[C_2mim][OAc]	$C_8H_{14}N_2O_2$	170.21	143314–17-4	Iolitec	>95%
1-butyl-3-methylimidazolium acetate	[C_4mim][OAc]	$C_{10}H_{18}N_2O_2$	198.26	284049–75-8	Sigma-Aldrich	≥95%
1-ethyl-3-methylimidazolium thiocyanate	[C_2mim][SCN]	$C_7H_{11}N_3S$	169.25	331717–63-6	Iolitec	>98%

Table 2
Water mass fraction (w_{H2O}), density (ρ), and refractive index (n_D) at 298.15 K and 101 kPa, experimentally measured in this work ("exp.") and taken from the literature ("lit.") [15–18], for the compounds involved in the studied systems.[a]

Compound	w_{H2O}	ρ/g·cm^{-3}		n_D	
	exp.	exp.	lit.	exp.	lit.
Acetone	0.0008	0.7848	0.78440	1.35595	1.35596
Water	–	0.9970	0.9970474	1.33258	1.33250
[C_2mim][OAc]	0.0012	1.0990	1.09989	1.50069	1.5005
[C_4mim][OAc]	0.0011	1.0508	1.0526	1.49490	1.49488
[C_2mim][SCN]	0.0006	1.1151	1.11170	1.55065	1.55064

[a] Uncertainties for density measurements: $u(T)$ = 0.1 K, $u(P)$ = 5 kPa, $u(\rho)$ = 0.0001 g/cm^3. Uncertainties for refractive index measurements: $u(T)$ = 0.02 K, $u(P)$ = 5 kPa, $u(n_D)$ = 0.00004.

The binary interaction parameters of this model were obtained from the correlation of the experimentally determined VLE data.

A flash unit was selected to carry out the recovery of each IL from its mixtures with acetone or water, on the basis of the non-volatile character of the ILs. A depiction of the simulation flowsheet is shown in Fig. 1. The feed flowrate introduced to the unit was set to 1000 kg·h^{-1} in all simulations, with a composition of 0.50 in mass fraction of IL, at 298.15 K and 101.32 kPa. The operation pressure of the flash tank was set to 101.32, 75, 50, 25, and 5 kPa. The energy requirements were supplied at two different points in the process: before the flash tank, by means of a heater; and directly in the flash tank, in order to reach the desired operation temperature. In all the simulations, it was ensured that the temperature was kept below levels at which substantial thermal decomposition would occur. In particular, the 5% onset decomposition temperatures of the different ILs at atmospheric pressure (427 K for [C_2mim][OAc] and 445 K for [C_4mim][OAc] [25]; and 476 K for [C_2mim][SCN] as specifically determined herein by thermogravimetric analysis at a heating rate of 5 K/min under nitrogen atmosphere) were considered in establishing the maximum tolerable temperatures.

3. Results and discussion

From the six binary systems resulting from the combination of the proposed molecular solvents (acetone or water) and ILs ([C_2mim][SCN], [C_2mim][OAc], or [C_4mim][OAc]), the isobaric VLE for the system water + [C_2mim][SCN] was previously studied and reported in the literature [26]. In the development of the study of the VLE of the other five systems, and as commented in Section 3.2 below, it was found that a vapour-liquid–liquid equilibrium (VLLE) actually existed for the system acetone + [C_2mim][OAc]. Due to its more complicated behaviour, this system will be the object of a separate work with a deeper thermodynamic focus. Thus, this work concentrates on the following systems: acetone + [C_2mim][SCN], acetone + [C_4mim][OAc], water + [C_2mim][OAc], and water + [C_4mim][OAc].

3.1. Physical properties

A number of physical properties were determined for the studied binary systems at 298.15 K and atmospheric pressure, namely: density (ρ), speed of sound through them (c), and refractive index (n_D). These are reported in Table 3 for the systems acetone + ([C_2mim][SCN] or [C_4mim][OAc]), and in Table 4 for the systems water + ([C_2mim][OAc] or [C_4mim][OAc]), covering the entire composition range. While in the systems with acetone all three properties increase with an increase of the IL concentration from pure acetone to pure IL, in the systems with water this is only the case for the refractive index. The density and speed of sound in both binary systems water + [C_2mim][OAc] and water + [C_4mim][OAc] exhibit maxima at some intermediate compositions. The evolution of these properties with the composition is more clearly observed in Figs. 2 and 3, where it is evident that ρ for the two systems of water with the acetate ILs exhibits a maximum at a water mole fraction of ca. 0.60–0.70. For those same systems, the maximum for c was recorded for the sample with a water mole fraction of ca. 0.90, although the maximum might well lie anywhere in the range 0.90–1.00, as no sample of composition in such range was investigated. In the literature, values by other authors for the den-

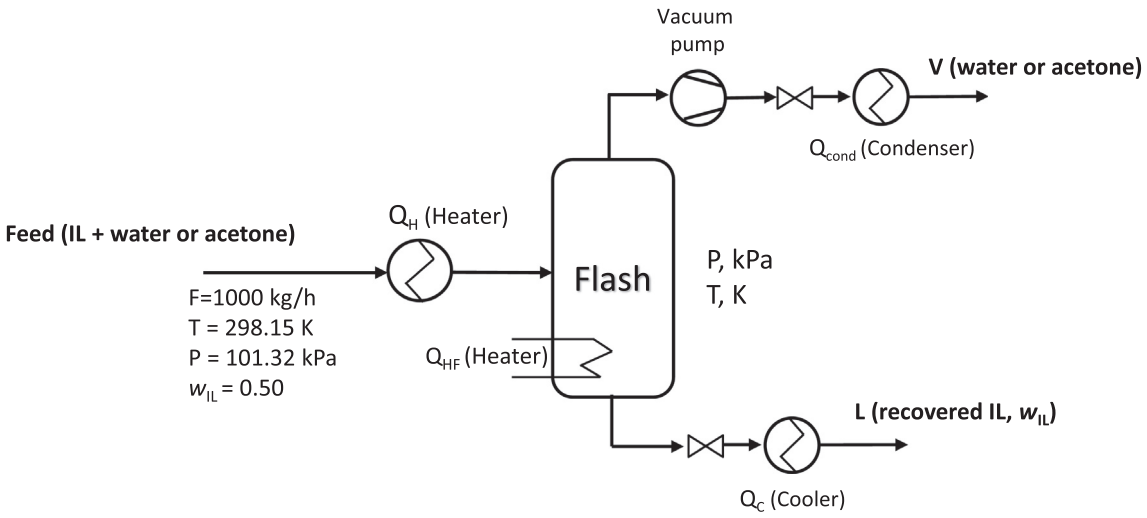

Fig. 1. Process flowsheet scheme for simulation of the IL recovery in Aspen Plus.

Table 3
Density (ρ), speed of sound (c), refractive index (n_D), excess molar volume (V^E), change of isentropic compressibility by mixing ($\Delta\kappa_s$), and change of molar refraction by mixing (ΔR_M), at 298.15 K and atmospheric pressure, for the binary systems acetone (1) + ([C_4mim][OAc] or [C_2mim][SCN]) (2). The compositions are expressed as mole fractions of acetone (x_1).[a]

x_1	ρ/g·cm^{-3}	c/m·s^{-1}	n_D	V^E/cm^3·mol^{-1}	$\Delta\kappa_s$/TPa^{-1}	ΔR_M/cm^3·mol^{-1}
Acetone (1) + [C_4mim][OAc] (2)						
0.0000	1.0508	1650	1.49490	0.000	0	0.000
0.1090	1.0414	1624	1.49033	−0.471	−13	0.050
0.2024	1.0318	1600	1.48559	−0.816	−25	0.088
0.3155	1.0183	1566	1.47864	−1.232	−40	0.110
0.3988	1.0062	1537	1.47230	−1.467	−51	0.117
0.4900	0.9899	1497	1.46364	−1.593	−61	0.116
0.5915	0.9685	1445	1.45222	−1.753	−70	0.106
0.6890	0.9421	1384	1.43825	−1.744	−71	0.097
0.8036	0.9010	1301	1.41651	−1.510	−59	0.073
0.8357	0.8868	1276	1.40886	−1.382	−52	0.056
1.0000	0.7848	1163	1.35595	0.000	0	0.000
Acetone (1) + [C_2mim][SCN] (2)						
0.0000	1.1151	1851	1.55065	0.000	0	0.000
0.1125	1.1020	1824	1.54287	−0.795	−28	0.050
0.1889	1.0899	1798	1.53596	−1.067	−47	0.100
0.3058	1.0722	1758	1.52501	−1.849	−79	0.116
0.3917	1.0558	1720	1.51465	−2.256	−103	0.108
0.5127	1.0280	1652	1.49785	−2.710	−134	0.125
0.6000	1.0031	1590	1.48270	−2.884	−153	0.120
0.6892	0.9725	1513	1.46416	−2.926	−164	0.106
0.7842	0.9307	1417	1.43948	−2.608	−159	0.093
0.9008	0.8642	1286	1.40112	−1.754	−113	0.069
1.0000	0.7848	1166	1.35595	0.000	0	0.000

[a] Uncertainties: $u(x)$ = 0.0002, $u(P)$ = 5 kPa, $u(\rho)$ = 0.0001 g·cm^{-3}, $u(T_\rho)$ = 0.1 K, $u(c)$ = 1 m·s^{-1}, $u(T_c)$ = 0.1 K, $u(n_D)$ = 0.00004, $u(T_{nD})$ = 0.02 K.

Table 4
Density (ρ), speed of sound (c), refractive index (n_D), excess molar volume (V^E), change of isentropic compressibility by mixing ($\Delta\kappa_s$), and change of molar refraction by mixing (ΔR_M), at 298.15 K and atmospheric pressure, for the binary systems water (1) + ([C_2mim][OAc] or [C_4mim][OAc]) (2). The compositions are expressed as mole fractions of water (x_1).[a]

x_1	ρ/g·cm^{-3}	c/m·s^{-1}	n_D	V^E/cm^3·mol^{-1}	$\Delta\kappa_s$/TPa^{-1}	ΔR_M/cm^3·mol^{-1}
Water (1) + [C_2mim][OAc] (2)						
0.0000	1.0990	1735	1.50069	0.000	0	0.000
0.1306	1.1006	1754	1.49883	−0.408	−10	−0.037
0.2326	1.1018	1763	1.49676	−0.699	−15	−0.071
0.2865	1.1036	1781	1.49605	−0.958	−23	−0.087
0.3671	1.1049	1795	1.49405	−1.169	−31	−0.097
0.4047	1.1055	1803	1.49276	−1.253	−35	−0.107
0.4896	1.1068	1811	1.48962	−1.433	−42	−0.113
0.5258	1.1072	1838	1.48758	−1.488	−52	−0.127
0.5507	1.1076	1841	1.48619	−1.532	−54	−0.132
0.6155	1.1079	1872	1.48192	−1.587	−68	−0.128
0.7151	1.1057	1910	1.47153	−1.536	−88	−0.117
0.7317	1.1055	1922	1.47061	−1.541	−93	−0.083
0.8099	1.0986	1952	1.45529	−1.342	−112	−0.075
0.9053	1.0718	1915	1.41896	−0.769	−125	−0.040
1.0000	0.9970	1495	1.33258	0.000	0	0.000
Water (1) + [C_4mim][OAc] (2)						
0.0000	1.0508	1650	1.49490	0.000	0	0.000
0.1109	1.0517	1655	1.49321	−0.248	−3	−0.043
0.2026	1.0529	1664	1.49206	−0.494	−7	−0.047
0.2683	1.0543	1672	1.49085	−0.722	−12	−0.081
0.4150	1.0576	1692	1.48785	−1.139	−25	−0.099
0.5113	1.0601	1715	1.48476	−1.359	−38	−0.110
0.6166	1.0621	1741	1.47932	−1.453	−52	−0.107
0.6604	1.0635	1760	1.47595	−1.511	−62	−0.124
0.6842	1.0640	1770	1.47390	−1.518	−67	−0.123
0.7104	1.0642	1780	1.47093	−1.499	−72	−0.130
0.7985	1.0632	1819	1.45815	−1.342	−93	−0.101
0.8964	1.0530	1855	1.42833	−0.902	−118	−0.057
1.0000	0.9970	1495	1.33258	0.000	0	0.000

[a] Uncertainties: $u(x)$ = 0.0002, $u(P)$ = 5 kPa, $u(\rho)$ = 0.0001 g·cm^{-3}, $u(T_\rho)$ = 0.1 K, $u(c)$ = 1 m·s^{-1}, $u(T_c)$ = 0.1 K, $u(n_D)$ = 0.00004, $u(T_{nD})$ = 0.02 K.

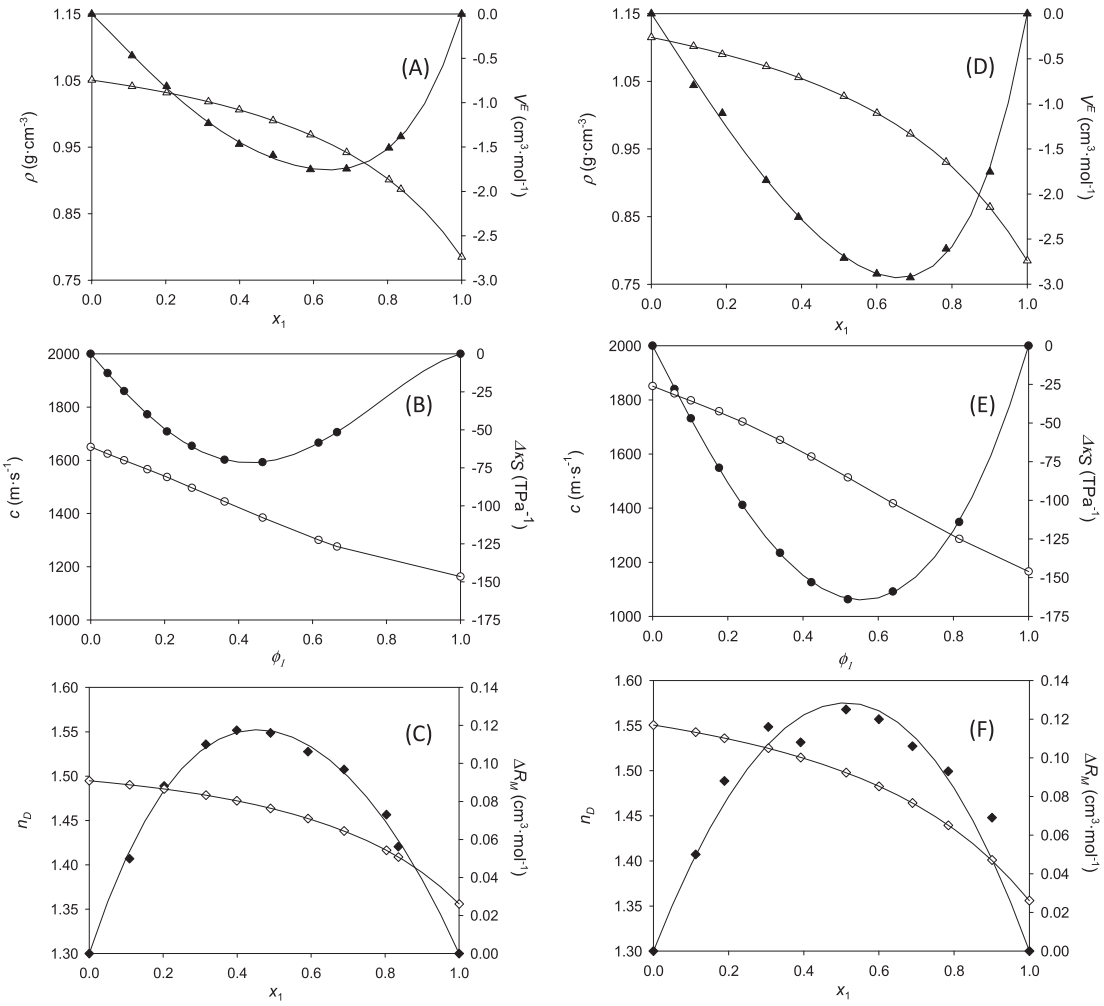

Fig. 2. Density (ρ, open triangles), speed of sound (c, open circles), refractive index (n_D, open diamonds), excess molar volume (V^E, solid triangles), change of isentropic compressibility by mixing ($\Delta\kappa_s$, solid circles), and change of molar refraction by mixing (ΔR_M, solid diamonds) at 298.15 K and atmospheric pressure for the systems acetone + [C_4mim][OAc] (plots A, B, and C on the left) and acetone + [C_2mim][SCN] (plots D, E, and F on the right) as a function of the mole fraction (x_1) or the volume fraction (ϕ_1) of acetone. Solid lines correspond to the correlations by Redlich-Kister polynomial fits of the derived properties.

sity of the system water + [C_2mim][OAc] at 298.2 K and atmospheric pressure were found [27,28], and are also displayed in plot A of Fig. 3 for direct visual comparison. An excellent agreement is observed with the data by Quijada-Maldonado et al. [27], whereas a good match can be also identified in the case of the data set reported by Anantharaj and Banerjee if taking into account their reported uncertainty and disregarding an individual data point far off the trend and probably due to a typing mistake in their article [28]. (For a straightforward visual comparison of the magnitude of the investigated properties across the acetone- and water-containing systems, the same axis scales were used in Figs. 2 and 3 for any given property.)

Finer precision in compositional analyses by physical property measurements can be achieved if using excess properties and changes of property by mixing. Thus, the excess molar volume (V^E), the change of isentropic compressibility by mixing ($\Delta\kappa_S$), and the change of molar refraction by mixing (ΔR_M) were calculated from the experimental values of ρ, c, and n_D, by means of the following expressions:

$$V^E = \frac{x_1 \cdot M_1 + x_2 \cdot M_2}{\rho} - \left(\frac{x_1 \cdot M_1}{\rho_1} + \frac{x_2 \cdot M_2}{\rho_2}\right) \quad (1)$$

$$\Delta\kappa_S = \kappa_S - (\phi_1 \cdot \kappa_{s,1} + \phi_2 \cdot \kappa_{s,2}) \quad (2)$$

$$\Delta R_M = R_M - (x_1 \cdot R_{M,1} + x_2 \cdot R_{M,2}) \quad (3)$$

where x_i and M_i are respectively the mole fraction and the molar mass of component i; subscripts 1 and 2 refer to the components in the binary mixture; ϕ_i represents the volume fraction of component i in the mixture:

$$\phi_i = \frac{x_i \cdot V_i}{x_1 \cdot V_1 + x_2 \cdot V_2} \quad (4)$$

and the isentropic compressibility (κ_S) and the molar refraction (R_M) were calculated as:

$$\kappa_S = \frac{1}{c^2 \cdot \rho} \quad (5)$$

$$R_M = \frac{n_D^2 - 1}{n_D^2 + 2} \cdot \frac{x_1 \cdot M_1 + x_2 \cdot M_2}{\rho} \quad (6)$$

The numerical values of V^E, $\Delta\kappa_S$, and ΔR_M are included in Table 3 and 4, and their evolution with the concentration is graphically shown in Fig. 2 for the systems with acetone and in Fig. 3 for the systems with water. Regarding V^E, negative values are obtained for all four systems over the entire composition range, with minima located roughly at a water or acetone mole fraction of 0.60–0.70. The relatively high absolute values of these minima (ranging

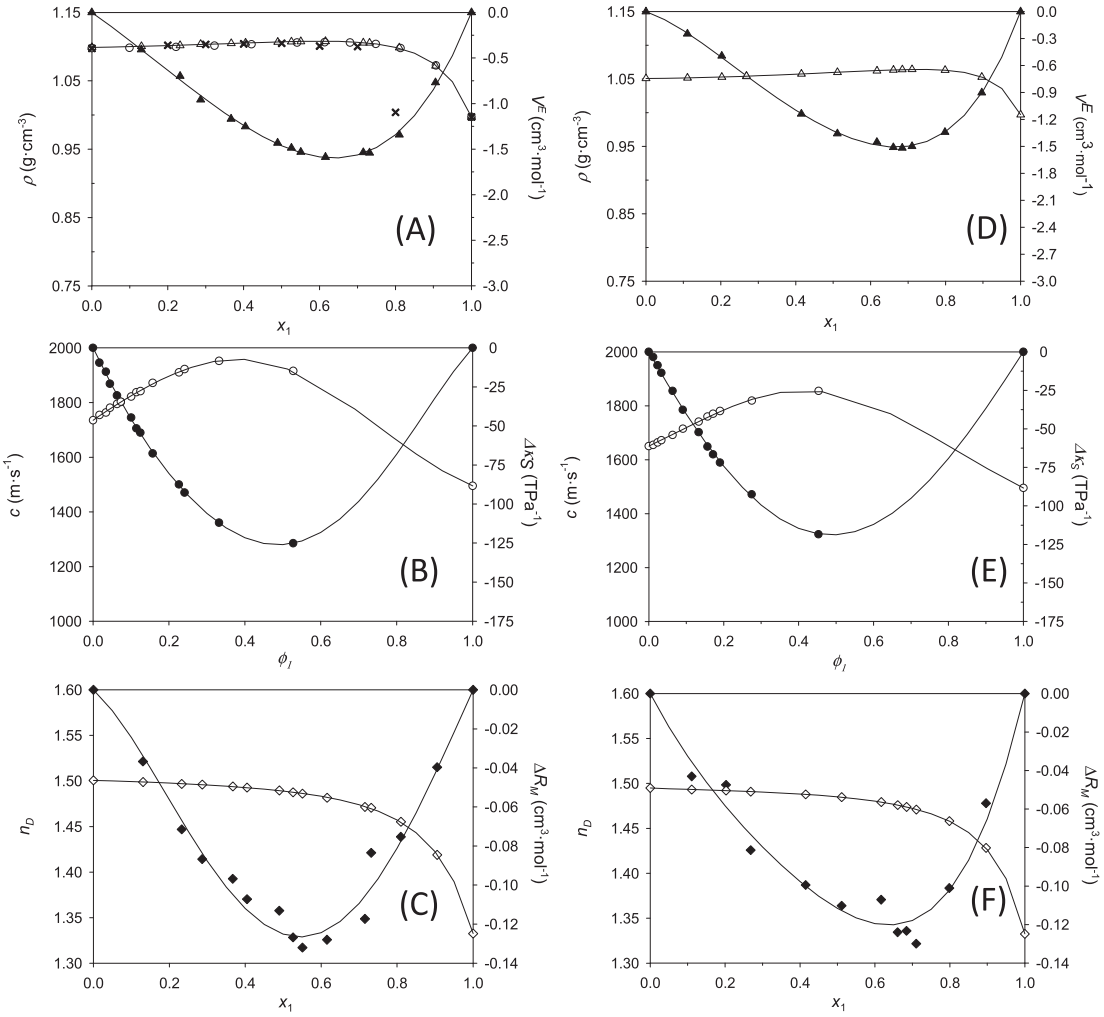

Fig. 3. Density (ρ, open triangles), speed of sound (c, open circles), refractive index (n_D, open diamonds), excess molar volume (V^E, solid triangles), change of isentropic compressibility by mixing ($\Delta\kappa_s$, solid circles), and change of molar refraction by mixing (ΔR_M, solid diamonds) at 298.15 K and atmospheric pressure for the systems water + [C_2mim][OAc] (plots A, B, and C on the left) and water + [C_4mim][OAc] (plots D, E, and F on the right) as a function of the mole fraction (x_1) or the volume fraction (ϕ_1) of water. Density literature data by Quijada-Maldonado et al. [27] (open squares) and by Anantharaj and Banerjee [28] (crosses) are also depicted in plot A. Solid lines correspond to the correlations by Redlich-Kister polynomial fits of the derived properties.

from 1.5 cm^3/mol to 2.9 cm^3/mol) are indicative of the existence of strongly attractive intermolecular interactions between the investigated ILs and either acetone or water (for example via establishment of hydrogen bonding [29]), but also of efficient molecular packing between the ions and molecules of the compounds involved. Negative values are also found for $\Delta\kappa_S$ for all compositions specifically explored, although no good coverage of the entire composition range is available with the tested samples, in terms of volume fraction scale, due to the large difference in molar mass between the ILs and either acetone or water. In any case, since κ_S represents a tendency to be compressed upon an increase in pressure, the analogy of the trends of $\Delta\kappa_S$ in the studied systems with those of V^E invites to think of a facilitation of the compression of the liquid mixtures thanks to the strongly attractive intermolecular interactions referred above. Curiously, ΔR_M presents positive values throughout the entire composition range in the systems with acetone, with maxima of ca. 0.12 $cm^3 \cdot mol^{-1}$ in the acetone mole fraction range of ca. 0.40–0.50; whereas negative values are observed in the systems with water, displaying minima of ca. –0.13 $cm^3 \cdot mol^{-1}$ in the water mole fraction range of ca. 0.50–0.70. The reasons for this opposite behaviour are unclear for us, but they may be related to the difference in polarisability of acetone and water, and how it is affected in each case by the presence of the ionic liquid.

The data sets of V^E, $\Delta\kappa_S$, and ΔR_M were correlated by means of Redlich-Kister polynomials [30] to enable a continuous mathematical description of their behaviour and facilitate their potential utilisation as calibration curves in the compositional analysis of samples of the studied systems. For V^E or ΔR_M of binary mixtures, the mathematical expression of the Redlich-Kister polynomials is:

$$\xi = x_1 \cdot x_2 \cdot \sum_{k=0}^{m} \left[A_k \cdot (x_1 - x_2)^k \right] \tag{7}$$

where ξ represents the excess property or change of property by mixing (i.e. V^E or ΔR_M), x_1 and x_2 are the mole fractions of components 1 and 2 of the binary mixture, and k is a void counter also serving as identifier of the m + 1 polynomial coefficients A_k to be fit. In the case of $\Delta\kappa_S$, based on a concentration scale in volume fractions, the analogous Redlich-Kister polynomial expression is:

$$\xi = \phi_1 \cdot \phi_2 \cdot \sum_{k=0}^{m} \left[A_k \cdot (\phi_1 - \phi_2)^k \right] \tag{8}$$

with ξ now being $\Delta\kappa_S$, and with ϕ_1 and ϕ_2 representing respectively the volume fractions of components 1 and 2. The A_k coefficients for all three derived properties were obtained by least-squares regression, with the final degree m of the fit polynomial being assessed through application of Fishers's F statistical test. Table 5 lists the coefficients of the correlation of V^E, $\Delta\kappa_S$, and ΔR_M data for all the studied systems, together with the corresponding standard deviation (σ) and relative standard deviation (σ_{rel}), calculated as:

$$\sigma = \sqrt{\frac{1}{n_{dat} - n_{par}} \cdot \sum_{i=1}^{n_{dat}} \left(\xi_{i,exp} - \xi_{i,calc}\right)^2} \tag{9}$$

$$\sigma_{rel} = \sqrt{\frac{1}{n_{dat} - n_{par}} \cdot \sum_{i=1}^{n_{dat}} \left(\frac{\xi_{i,exp} - \xi_{i,calc}}{\xi_{i,calc}}\right)^2} \tag{10}$$

where n_{dat} is the total number of experimental data ξ_i in the set to be correlated, n_{par} is the number of fit parameters, and subscripts *exp* and *calc* refer respectively to the experimental and calculated values. The resulting fits are plotted in Figs. 2 and 3. Althout the description provided by the Redlich-Kister polynomials for ΔR_M is acceptable, it is particularly excellent for V^E and $\Delta\kappa_S$, as corroborated numerically by the values of σ_{rel} shown in Table 5. With the σ_{rel} value of its correlations lower than 0.05 for any of the studied systems, the V^E (and hence density) was selected as the property of reference for the compositional analysis of the equilibrated samples of the VLE experiments.

3.2. Vapour-liquid equilibria and data correlation

The isobaric VLE data of the binary systems acetone + ([C_4mim][OAc] or [C_2mim][SCN]) and water + ([C_2mim][OAc] or [C_4mim][OAc]), experimentally determined at absolute pressures of 101.32, 50.00, and 30.00 kPa (for the systems with acetone) or 25.00 kPa (for the systems with water), are listed in Tables 6 and 7. Only the boiling temperature and liquid composition are specified for each experimental data point, as the vapour phase in equilibrium is constituted by pure acetone or pure water due to the negligible volatility of the ILs at the experimental conditions of pressure and temperature investigated. This was assumed a priori, but it was also checked occasionally for random samples of the condensed vapour phases during the experimental determination of the VLE of the different systems, verifying that the density of these samples was indeed corresponding to that of pure acetone or of pure water.

From inspection of the values in Tables 6 and 7, and as expected, it is clear that the boiling temperature (bubble temperature) of the mixtures increases with a reduction in the mole fraction of acetone or water in the liquid phase; or, equivalently, with an increase of the overall composition of ionic liquid in the system. The data sets did not cover the part of the compositional spectrum with the greatest IL concentrations because of the thermal decomposition of the ILs that would occur before the boiling of the mixtures.

Figs. 4 and 5 show the temperature-composition isobaric diagrams (just the liquid saturation lines) for the systems studied, for which it is clear that a reduction in the absolute pressure leads to a reduction of the boiling temperature at any given composition. Besides that, in Fig. 4 it is interesting to observe that the increase in boiling temperature caused at a given pressure by an increase in the concentration of IL is quite similar in both systems. However, this must not lead to the assumption that the variation of the boiling temperature of systems acetone + IL with the composition is independent of the IL nature. A preliminary investigation of the VLE of the binary system acetone + [C_2mim][OAc] (an IL that only differs with [C_4mim][OAc] in the length of one of the alkyl substituents, and which shares with [C_2mim][SCN] not only the same cation but also a relatively small anion with basic character) has resulted in the identification of a liquid–liquid equilibrium domain intersecting with the vapour-liquid equilibrium domain. Thus, even small variations in the chemical structure of the IL can have a very significant influence in the phase behaviour of acetone + IL systems. The particular liquid–liquid-vapour equilibrium behaviour of acetone + [C_2mim][OAc] will be the object of further and detailed analysis in a separate work in the future.

In Fig. 5, the increase in boiling temperature for each isobar with an increase of the IL concentration is also reasonably similar between the two water + IL systems, particularly in the case of atmospheric pressure. At the sub-atmospheric pressures, a slightly higher pace of increase of the boiling temperature can be noticed for the system with [C_2mim][OAc]. This effect has to be necessarily attributed to the shorter alkyl substituent chain in the IL cation, which is the only difference in terms of chemical structure between [C_2mim][OAc] and [C_4mim][OAc]. An analysis of the effect of the nature of the anion can be made by direct comparison of the VLE at atmospheric pressure for the systems water + [C_2mim][OAc] (this work) and water + [C_2mim][SCN] (taken from the literature [26]) – see Fig. S7 in the Supplementary Material. This comparison

Table 5
Coefficients A_k of the Redlich-Kister polynomials, along with the corresponding standard deviations (σ) and relative standard deviations (σ_{rel}), for the correlation of the excess molar volume V^E, the change of isentropic compressibility by mixing $\Delta\kappa_S$, and the change of molar refraction by mixing (ΔR_M) of the binary systems acetone + ([C_4mim][OAc] or [C_2mim][SCN]) and water + ([C_2mim][OAc] or [C_4mim][OAc]) at 298.15 K and atmospheric pressure. (The values of σ are expressed in the same units as those indicated for the corresponding property in the first column.)

Property	A_0	A_1	A_2	A_3	σ	σ_{rel}
Acetone + [C_4mim][OAc]						
V^E/cm^3·mol^{-1}	−6.568	−3.054	−2.163	−1.602	0.019	0.017
$\Delta\kappa_s$/TPa^{-1}	−279	110	101	–	<1	0.010
ΔR_M/cm^3·mol^{-1}	0.467	−0.0795	0.0461	–	0.003	0.048
Acetone + [C_2mim][SCN]						
V^E/cm^3·mol^{-1}	−10.61	−6.176	−3.840	−2.045	0.044	0.041
$\Delta\kappa_s$/TPa^{-1}	−649	−150	−5.17	−31.2	<1	0.010
ΔR_M/cm^3·mol^{-1}	0.411	0.154	0.424	–	0.015	0.172
Water + [C_2mim][OAc]						
V^E/cm^3·mol^{-1}	−5.850	−3.597	−0.9079	−0.2239	0.028	0.030
$\Delta\kappa_s$/TPa^{-1}	−504	31.0	111	93.1	1	0.046
ΔR_M/cm^3·mol^{-1}	−0.491	−0.118	0.170	–	0.009	0.089
Water + [C_4mim][OAc]						
V^E/cm^3·mol^{-1}	−5.307	−3.882	−1.213	−1.267	0.014	0.018
$\Delta\kappa_s$/TPa^{-1}	−475	26.1	73.7	–	1	0.110
ΔR_M/cm^3·mol^{-1}	−0.4463	−0.2271	−0.1504	–	0.009	0.095

Table 6
Experimental isobaric vapour-liquid equilibrium data for the binary systems acetone + [C_4mim][OAc] and acetone + [C_2mim][SCN] at 101.32, 50.00, and 30.00 kPa. Only the acetone mole fraction of the liquid phase in equilibrium (x_1) is shown, since the acetone mole fraction of the vapour phase in equilibrium (y_1) is equal to 1.000 in all cases due to the non-volatile character of the ionic liquids at the experimental conditions of pressure (P) and temperature (T) investigated herein.[a]

P = 101.32 kPa		P = 50.00 kPa		P = 30.00 kPa	
T/K	x_1	T/K	x_1	T/K	x_1
Acetone (1) + [C_4mim][OAc] (2)					
329.2	1.000	310.2	1.000	297.7	1.000
329.4	0.988	310.4	0.941	297.7	0.989
329.6	0.973	310.7	0.881	297.7	0.976
329.9	0.948	311.4	0.795	297.8	0.969
330.4	0.905	311.9	0.755	297.8	0.942
330.8	0.873	313.8	0.708	297.9	0.928
331.2	0.838	314.9	0.669	297.9	0.905
332.3	0.790	315.6	0.632	298.0	0.879
332.9	0.757	316.7	0.613	298.2	0.838
333.7	0.723	319.0	0.590	298.5	0.791
334.8	0.683	326.3	0.455	299.6	0.747
336.1	0.648	331.0	0.398	299.9	0.726
339.7	0.548	334.7	0.348	300.4	0.697
343.7	0.476	340.0	0.305	301.1	0.666
344.6	0.468			301.9	0.638
347.2	0.449			303.7	0.598
350.6	0.412			304.2	0.594
356.3	0.377			306.6	0.554
361.0	0.338			308.4	0.521
370.7	0.300			310.8	0.486
373.8	0.281			316.9	0.401
378.5	0.254			321.0	0.355
383.2	0.238				
388.1	0.219				
Acetone (1) + [C_2mim][SCN] (2)					
329.2	1.000	310.2	1.000	297.7	1.000
330.0	0.949	310.2	0.990	297.7	0.999
330.5	0.910	310.5	0.969	298.2	0.968
330.8	0.876	310.7	0.956	298.6	0.931
330.9	0.863	310.9	0.935	298.9	0.868
331.3	0.820	311.3	0.893	299.5	0.839
333.1	0.693	311.7	0.850	299.6	0.800
333.3	0.686	311.9	0.819	299.7	0.797
333.6	0.675	312.3	0.786	300.1	0.751
335.1	0.616	312.6	0.756	300.5	0.722
337.6	0.542	313.0	0.732	301.3	0.677
338.4	0.526	313.7	0.684	301.8	0.649
339.9	0.495	314.3	0.660	302.3	0.628
340.6	0.477	314.7	0.640	303.0	0.605
341.8	0.460	316.1	0.586	304.0	0.568
355.0	0.332	317.4	0.549	308.3	0.457
355.9	0.319	318.5	0.519	310.0	0.419
362.9	0.278	322.9	0.429	311.3	0.402
369.9	0.241	324.4	0.406	315.4	0.344
387.8	0.170	326.3	0.393	317.8	0.327
393.2	0.134	328.7	0.373	318.6	0.319
		330.3	0.364	325.5	0.254
		341.9	0.287	335.1	0.194
		358.6	0.180	343.1	0.150
		370.2	0.131	351.1	0.119

[a] Uncertainties: $u(T)$ = 0.1 K, $u(P)$ = 0.005 kPa, $u(x)$ = 0.001.

shows that, from the boiling of pure water, the bubble temperature of the mixture raises at a substantial higher pace in the case of the system with the acetate-containing IL; probably due to a stronger interaction between the acetate anions and the water molecules (relative to the thiocyanate-water interaction).

A comparison of the systems acetone + [C_4mim][OAc] and water + [C_4mim][OAc] is also possible, revealing the effect of the nature of the molecular solvent (acetone or water) in their VLE. By simultaneous consideration of the plot on the left of Fig. 4 and the plot on the right of Fig. 5, it can be seen that, for equivalent concentrations of IL, the increase in boiling temperature of the mixture with regard to the pure molecular solvent is much higher in the case of the system with water. This is likely due to the existence of a much stronger hydrogen bonding between water and the IL (particularly the acetate anion) than between acetone and the IL.

A further interesting comparison is that of the systems acetone + [C_2mim][SCN] (this work) and water + [C_2mim[SCN] (taken from the literature [26]) at atmospheric pressure, also evidenced in Fig. S7 in the Supplementary Material. This comparison shows a relatively mild increase of the bubble temperature (with respect to the pure molecular solvent) in both systems as the concentration of IL is increased. No special difference in the pace of this increase is noticeable, suggesting a more equilibrated interaction

Table 7
Experimental isobaric vapour-liquid equilibrium data for the binary systems water + [C_2mim][OAc] and water + [C_4mim][OAc] at 101.32, 50.00, and 25.00 kPa. Only the water mole fraction of the liquid phase in equilibrium (x_1) is shown, since the water mole fraction of the vapour phase in equilibrium (y_1) is equal to 1.000 in all cases due to the non-volatile character of the ionic liquids at the experimental conditions of pressure (P) and temperature (T) investigated herein.[a]

P = 101.32 kPa		P = 50.00 kPa		P = 25.00 kPa	
T/K	x_1	T/K	x_1	T/K	x_1
Water (1) + [C_2mim][OAc] (2)					
373.2	1.000	354.5	1.000	338.3	1.000
376.9	0.952	357.9	0.961	338.3	0.997
378.8	0.936	359.6	0.946	338.5	0.994
382.4	0.908	361.9	0.930	338.7	0.990
385.1	0.890	364.3	0.912	339.2	0.985
388.3	0.869	366.0	0.896	339.7	0.978
390.8	0.853	367.1	0.889	341.4	0.960
393.9	0.835	368.9	0.876	343.2	0.943
396.6	0.820	372.4	0.853	345.5	0.924
399.9	0.802	376.9	0.827	348.5	0.902
403.0	0.796	381.5	0.800	352.1	0.875
405.1	0.786	386.9	0.771	359.0	0.833
408.5	0.767	391.1	0.750	365.6	0.794
411.9	0.750	396.7	0.730	373.4	0.755
414.5	0.740	401.7	0.714	377.6	0.735
418.6	0.721	406.7	0.700	382.9	0.712
		411.7	0.693	390.0	0.685
		416.6	0.669	394.9	0.676
Water (1) + [C_4mim][OAc] (2)					
373.2	1.000	354.5	1.000	338.3	1.000
376.9	0.951	358.0	0.951	338.5	0.995
379.4	0.927	360.3	0.927	339.4	0.979
382.6	0.902	364.0	0.894	341.0	0.958
385.6	0.880	368.5	0.861	342.7	0.937
387.1	0.871	374.0	0.828	346.3	0.890
388.6	0.861	378.9	0.803	350.1	0.867
391.6	0.845	383.5	0.778	355.2	0.828
394.7	0.825	390.6	0.706	360.1	0.810
397.8	0.810	395.3	0.684	362.5	0.801
401.2	0.794	399.6	0.670	368.2	0.766
404.0	0.790	402.8	0.653	371.6	0.747
407.1	0.770	406.0	0.643	378.6	0.699
409.3	0.763	407.9	0.638	383.7	0.664
412.7	0.746	410.7	0.623	388.7	0.637
416.3	0.722	419.9	0.576	396.8	0.562
421.4	0.687			401.7	0.543
				405.6	0.522
				417.3	0.474

[a] Uncertainties: u(T) = 0.1 K, $u(P)$ = 0.005 kPa, u(x) = 0.001.

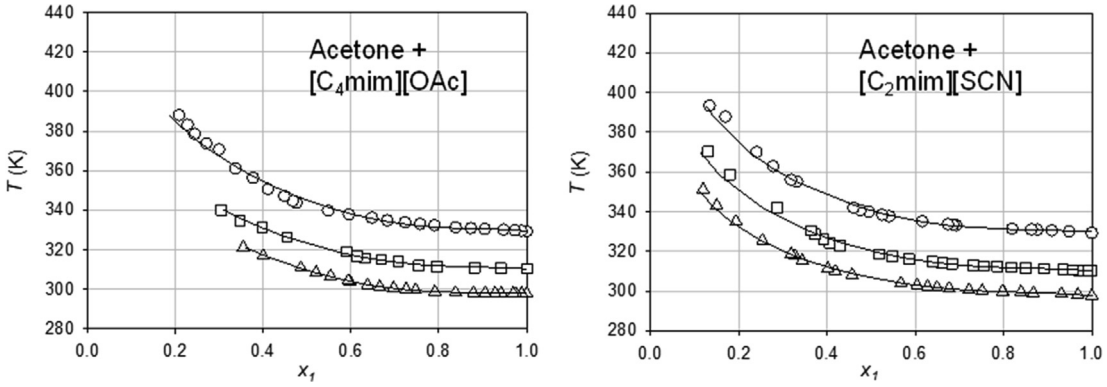

Fig. 4. Temperature-composition diagrams (liquid saturation lines) for the experimental VLE data of the binary systems acetone + [C_4mim][OAc] (left) and acetone + [C_2mim][SCN] (right) at 101.32 kPa (○), 50.00 kPa (□), and 30.00 kPa (Δ), as a function of the mole fraction of acetone (x_1). The vapour saturation lines are omitted, as they correspond to pure acetone (x_1 = 1.000) in all cases. NRTL correlations are plotted as solid lines.

of the thiocyanate anion with water and with acetone than the one of the acetate anion, which clearly exhibits a preferential interaction with water.

A non-linear regression method based on the maximum likelihood principle was used to perform the correlation of the experimental VLE data (pressure, temperature, and mole fractions of

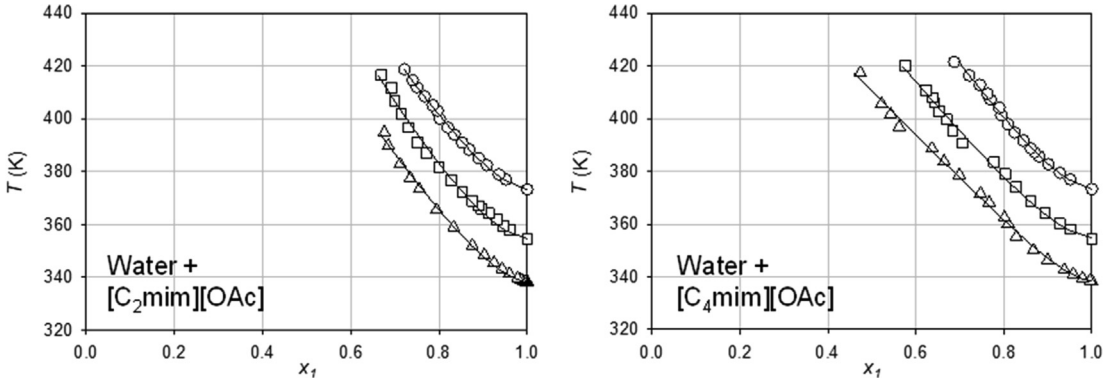

Fig. 5. Temperature-composition diagrams (liquid saturation lines) for the experimental VLE data of the binary systems water + [C_2mim][OAc] (left) and water + [C_4mim][OAc] (right) at 101.32 kPa (○), 50.00 kPa (□), and 25.00 kPa (Δ), as a function of the mole fraction of water (x_1). The vapour saturation lines are omitted, as they correspond to pure water (x_1 = 1.000) in all cases. NRTL correlations are plotted as solid lines.

the liquid and vapour phases) for all the investigated systems. Ideality was assumed for the vapour phase, as it was composed of only one component (either acetone or water). For calculation of the saturation pressures of the different compounds, Antoine's equation was used. The coefficients for the application of this equation were retrieved from the literature for acetone and water [31], whereas for the ILs they were arbitrarily set to fictional values leading to a negligible vapour pressure (see Table S2 in the Supplementary Material). The NRTL model [24] was used to calculate the activity coefficients of the liquid phases, with the non-randomness parameter α being set to different values (namely 0.10, 0.20, and 0.30), and selecting in each case the value leading to the best correlation of the corresponding experimental dataset. The binary interaction parameters obtained with this model are listed in Table 8, along with the standard deviations in temperature, in mole fractions of the liquid and vapour phase, and in pressure. The corresponding NRTL correlations are plotted in Figs. 4 and 5, where a satisfactory description of the experimental VLE data points can be visually confirmed, in line with the relatively low standard deviations also included in Table 8.

With the aim of obtaining more reliable software simulations in processes involving the VLE of the studied systems, across a certain range of pressures, the simultaneous NRTL correlation of the three VLE data isobars for each system was also carried out. The corresponding results are shown in Table 8 in the rows labelled as "all" in the far-left column (pressure). The standard deviations for these simultaneous correlations are also reported and are found to be comparable to those of the correlations of the individual sets at a single pressure, hence considered as satisfactory.

3.3. Process simulation

After suitable implementation in the simulation software of the binary interaction parameters resulting from the simultaneous correlation of the VLE data of the three experimental isobars available for each investigated system (see Section 3.2 above), simulations were run according to the flowsheet scheme in Fig. 1. The operating pressure P and temperature T of the flash tank were varied, while keeping constant the feed characteristics: 1000 kg·h^{-1} with an ionic liquid mass fraction $w_{IL,0}$ = 0.50, at 298.15 K and 101.32 kPa. For each run, the composition of the outlet liquid stream and the energy requirements (resulting from the sum of the heat flow rates labelled as Q_H and Q_{HF} in Fig. 1) were recorded. The energy associated with the operation of the vacuum pump for

Table 8
Binary interaction parameters (Δg_{12}, Δg_{21}) and standard deviations (σ) in temperature (T), liquid mole fraction (x), vapour mole fraction (y), and pressure (P), for the correlation of the VLE data with the NRTL model (using the indicated non-randomness parameter α), at each of the three investigated pressures, as well as considering all three investigated pressures together (rows labelled as "all" in the left column), for the four binary systems studied in this work.

P/kPa	α	Δg_{12}/J·mol^{-1}	Δg_{21}/J·mol^{-1}	$\sigma(T)$/K	$\sigma(x)$	$\sigma(y)$	$\sigma(P)$/kPa
Acetone (1) + [C_4mim][OAc] (2)							
101.32	0.10	24,028	−12375	0.3	0.017	0.001	0.06
50.00	0.10	21,735	−11217	0.3	0.005	0.001	0.04
30.00	0.10	23,017	−11405	0.2	0.002	0.001	0.01
all	0.10	22,917	−11704	0.4	0.013	0.001	0.01
Acetone (1) + [C_2mim][SCN] (2)							
101.32	0.10	20,969	−10506	0.3	0.009	0.001	0.03
50.00	0.10	19,436	−9881.2	0.3	0.011	0.000	0.05
30.00	0.10	17,172	−8866.0	0.2	0.005	0.000	0.04
all	0.20	12,331	−4837.0	0.3	0.011	0.000	0.06
Water (1) + [C_2mim][OAc] (2)							
101.32	0.10	8243.8	−24002	0.1	0.003	0.000	0.00
50.00	0.10	−2382.1	−22511	0.1	0.009	0.000	0.02
25.00	0.10	3504.0	−23376	0.1	0.006	0.000	0.03
all	0.10	3513.8	−23564	0.1	0.008	0.000	0.02
Water (1) + [C_4mim][OAc] (2)							
101.32	0.10	11,897	−24314	0.1	0.005	0.000	0.01
50.00	0.10	13,133	−22981	0.1	0.008	0.000	0.02
25.00	0.20	3492.3	−14831	0.1	0.008	0.001	0.04
all	0.20	4528.8	−15305	0.2	0.010	0.001	0.03

operation at sub-ambient pressures was neglected in the evaluation of these energy requirements. The results are displayed as surface responses in 3D plots in Fig. 6, where the upper ends of the temperature scales have been set at ca. 10 K below the 5% onset decomposition temperatures of the corresponding IL in each case (see Section 2.3). Simulations at pressures and temperatures out-

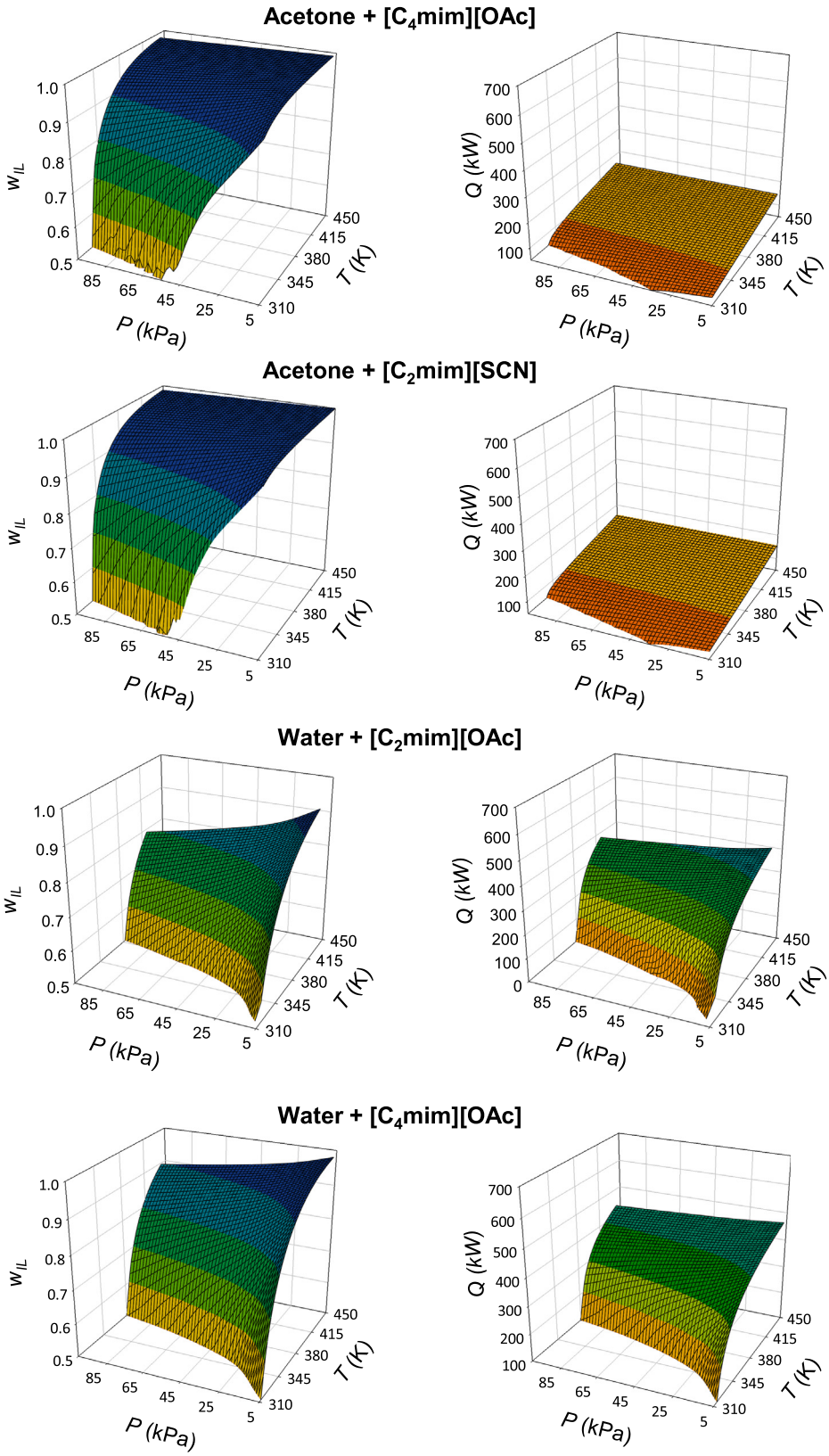

Fig. 6. IL mass fractions in the outlet IL-rich stream (w_{IL}), and required heat duties (Q), in the process (see scheme in Fig. 1) for regeneration of the ILs [C_2mim][SCN], [C_2mim][OAc], or [C_4mim][OAc] from their binary mixtures with acetone or water, as a function of the operating pressure (P) and temperature (T) in the flash tank.

side the range of data obtained experimentally should be taken with caution, as they are the result of extrapolating the NRTL correlations beyond the experimentally boundaries within which their parameters were obtained.

For the mixtures of acetone + ([C_4mim][OAc] or [C_2mim][SCN]), recovery of the IL with high purity ($\geq$0.98) was possible at atmospheric pressure only if reaching a minimum temperature of 420 K. This value is rather close to the 5% onset decomposition temperatures of the ILs. The same recovery purity could be achieved at somewhat lower temperatures by operating at reduced pressure. In the case of having the flash tank operating at 5 kPa, the corresponding temperatures would be: 330 K for the system with [C_4mim][OAc] and 315 K for the system with [C_2mim][SCN]. The energy requirements will be relatively low: less than 200 kW for any of the combinations of flash operating temperature and pressure evaluated.

Regarding the mixtures of water with the acetate-based ILs, an equivalent degree of purity in the recovered IL ($w_{IL} \geq 0.98$) could not be achieved for the system water + [C_2mim][OAc] even at the maximum acceptable temperature and the lowest pressure tested (P = 5 kPa), whereas for the system water + [C_4mim][OAc] a temperature as demanding as 415 K would be required at that pressure. By lowering the threshold to a more moderate recovery purity such as w_{IL} = 0.90, it is observed that this can still be barely achieved for the system with [C_2mim][OAc] (a temperature of 390 K will be needed if operating the flash tank at an absolute pressure of 5 kPa). For the system with [C_4mim][OAc], this IL mass fraction of 0.90 can be achieved at temperatures in the range 360–400 K if operating at pressures lower than 25 kPa; or alternatively under softer vacuum requirements if the operating temperature is increased (for instance, 435 K at an absolute pressure of 75 kPa). These slightly less demanding requirements for recovery of [C_4mim][OAc] from its mixtures with water (as compared to the case of [C_2mim][OAc]) may be related with the slightly lower absolute values of its excess molar volumes (see Table 4), which may be taken as a reflection of the intensity of the interaction that exists between water and the IL at a molecular level. In any case, both [C_2mim][OAc] and [C_4mim][OAc] interact strongly with water, and this leads unsurprinsingly to a relevant requirement of heat duty in performing the recovery of these ILs from their mixtures with water: for the target recovery purity of w_{IL} = 0.90 discussed above, energy requirements in the range 375–425 kW will be typically needed.

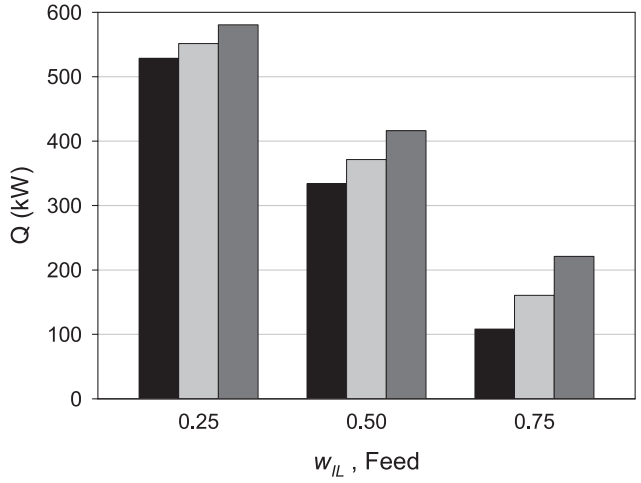

Fig. 7. Required heat duties (Q) for achieving an IL mass fraction of 0.80 (black columns), 0.85 (light grey columns), or 0.90 (dark grey columns) in the outlet IL-rich stream at an absolute pressure of 5 kPa in the flash tank, in the system water + [C_2-mim][OAc], for three different IL mass fractions in the feed stream: 0.25, 0.50, and 0.75.

It should be noted that the composition of the feed stream will not affect the VLE condition at which a given recovery purity is achieved, thus having only an influence in the heat duty required as a result of a larger amount of the molecular solvent to be vaporised. This is illustrated in particular for the system water + [C_2mim][OAc] in Fig. 7, where the energy required to achieve recovered IL purities of 0.80, 0.85, and 0.90 is represented for three different compositions of the feed stream ($w_{IL,0}$ = 0.25, 0.50, and 0.75) at the fixed operating pressure of 5 kPa. The variation of the values of Q for a given feed composition (representing the energy requirement for additional improvements of 0.05 in mass fraction in the purity of the recovered IL) is relatively small if compared to the variation between sets for the different feed compositions (with a step of 0.25 in $w_{IL,0}$).

4. Conclusions

The recovery with a good level of purity of the ILs [C_2mim][SCN], [C_2mim][OAc], or [C_4mim][OAc] from their mixtures with either acetone or water by flash distillation is not as straightforward as the nearly infinite relative volatility might suggest. This is in line with what was concluded in previous works on the recovery of some ILs from their mixtures with different molecular substances [11–13], inviting to think that it is a fact that can be generalised to a certain extent.

Experimental determination of the isobaric VLE data for the binary systems (water or acetone) + IL at three different pressures, with subsequent correlation by means of the NRTL equation, allowed the development of reliable simulations of a flash unit for their separation in the process simulation software Aspen Plus. The need of a notably reduced pressure in the flash tank, even if operating at temperatures close to those marking the limit of thermal stability of the ILs, was identified in these simulations. In the case of the systems acetone + ([C_4mim][OAc] or [C_2mim][SCN]), recovery purities of w_{IL} = 0.98 can be obtained in the IL-rich outlet stream at atmospheric pressure only at flash temperatures higher than 420 K. Application of vacuum, reducing the absolute pressure of the flash stage down to 5 kPa, allows a reduction of almost 100 K in the operating temperature if the same degree of purity is to be kept. For the systems involving water and the acetate-based ILs, the recovery purity of 0.98 is not achievable for [C_2mim][OAc] in the flash unit within the acceptable temperature ranges even at an operating pressure of 5 kPa; whereas for [C_4mim][OAc], a high operating temperature is needed at this same pressure. This difficulty in the separation of water and either of the acetate ILs correlates well with the strongly negative V^E values for the corresponding mixtures, which are indicative of the strong interaction existing between the water and IL species. For a significantly more modest recovery purity of w_{IL} = 0.90 in these acetate-containing systems, the separation process will still require a flash temperature of 350–400 K even if operating the flash tank under an absolute pressure as low as 5 kPa; with heat duty requirements in the range 375–425 kW. However, it should be noted that, in the real context of an IL recovery unit of this kind, energy integration would be possible by using the hot flash outlet streams to preheat the feed stream, thus reducing substantially the duty requirement.

CRediT authorship contribution statement

Nuria Caeiro: Formal analysis, Investigation. **Marta K. Wojtczuk:** Formal analysis, Investigation, Funding acquisition. **Héctor Rodríguez:** Conceptualization, Methodology, Validation, Writing

– original draft, Supervision, Visualization. **Eva Rodil:** Conceptualization, Methodology, Validation, Supervision, Visualization, Writing – review & editing. **Ana Soto:** Resources, Project administration, Funding acquisition, Writing – review & editing.

Declaration of Competing Interest

The authors declare that they have no known competing financial interests or personal relationships that could have appeared to influence the work reported in this paper.

Acknowledgements

The authors acknowledge Xunta de Galicia for support through project ED431B 2020/021. M.K.W. is grateful to the Erasmus + programme of the European Union for the award of a mobility traineeship.

Appendix A. Supplementary data

Supplementary data to this article can be found online at https://doi.org/10.1016/j.molliq.2021.118292.

References

[1] M. Freemantle, An Introduction to Ionic Liquids, RSC Publishing, Cambridge (UK), 2010.
[2] M.B. Shiflett (Ed.), Commercial Applications of Ionic Liquids, Springer, Cham (Switzerland), 2020.
[3] K.R. Seddon, Ionic liquids for clean technology, J. Chem. Technol. Biotechnol. 68 (1997) 351–356, https://doi.org/10.1002/(SICI)1097-4660(199704)68:4<351::AID-JCTB613>3.0.CO;2-4.
[4] A. Brandt, J. Gräsvik, J.P. Hallett, T. Welton, Deconstruction of lignocellulosic biomass with ionic liquids, Green Chem. 15 (2013) 550–583, https://doi.org/10.1039/c2gc36364j.
[5] A.M. da Costa Lopes, K.G. João, A.R.C. Morais, E. Bogel-Łukasik, R. Bogel-Łukasik, Ionic liquids as a tool for lignocellulosic biomass fractionation, Sustain. Chem. Process 1 (2013) 3, https://doi.org/10.1186/2043-7129-1-3.
[6] H. Rodríguez, Ionic liquids in the pretreatment of lignocellulosic biomass, Acta Innovations 38 (2021) 22–35, https://doi.org/10.32933/ActaInnovations.38.3.
[7] J.F. Fernández, J. Neumann, J. Thörning, Regeneration, recovery and removal of ionic liquids, Curr. Org. Chem. 15 (2011) 1992–2014, https://doi.org/10.2174/138527211795703676.
[8] D. Klein-Marcuschamer, B.A. Simmons, H.W. Blanch, Techno-economic analysis of a lignocellulosic ethanol biorefinery with ionic liquid pretreatment, Biofuel Bioprod. Biorefin. 5 (5) (2011) 562–569, https://doi.org/10.1002/bbb.303.
[9] Z. Usmani, M. Sharma, P. Gupta, Y. Karpichev, N. Gathergood, R. Bhat, V.K. Gupta, Ionic liquid based pretreatment of lignocellulosic biomass for enhanced bioconversion, Bioresour. Technol. 304 (2020) 123003, https://doi.org/10.1016/j.biortech.2020.123003.
[10] C. Wang, X. Luo, X. Zhu, G. Cui, D.-e. Jiang, D. Deng, H. Li, S. Dai, The strategies for improving carbon dioxide chemisorption by functionalized ionic liquids, RSC Adv. 3 (36) (2013) 15518, https://doi.org/10.1039/c3ra42366b.
[11] M.K. Wojtczuk, N. Caeiro, H. Rodríguez, E. Rodil, A. Soto, Recovery of the ionic liquids [C_2mim][OAc] or [C_2mim][SCN] by distillation from their binary mixtures with methanol or ethanol, Sep. Purif. Technol. 248 (2020) 117103, https://doi.org/10.1016/j.seppur.2020.117103.
[12] Z. Zhu, Y. Ri, M. Li, H. Jia, Y. Wang, Y. Wang, Extractive distillation for ethanol dehydration using imidazolium-based ionic liquids as solvents, Chem. Eng. Process. 109 (2016) 190–198, https://doi.org/10.1016/j.cep.2016.09.009.
[13] W. Li, Y. Zhang, L. Wang, H. Feng, T. Zhang, Evaluation of ionic liquid separation ability for the benzene-methanol mixture by extractive distillation, J. Chem. Technol. Biotechnol. 95 (2019) 1100–1109, https://doi.org/10.1002/jctb.6294.
[14] K.R. Seddon, A. Stark, M.-J. Torres, Influence of chloride, water, and organic solvents on the physical properties of ionic liquids, Pure Appl. Chem. 72 (2000) 2275–2287, https://doi.org/10.1351/pac200072122275.
[15] J.A. Riddick, W.B. Bunger, T. Sakano (Eds.), Organic Solvents, 4th ed., John Wiley, New York (USA), 1986.
[16] Q.G. Zhang, S.Y. Cai, W.B. Zhang, Y.L. Lan, X.Y. Zhang, Density, viscosity, conductivity, refractive index and interaction study of binary mixtures of the ionic liquid 1-ethyl-3-methylimidazolium acetate with methyldiethanolamine, J. Mol. Liq. 233 (2017) 471–478, https://doi.org/10.1016/j.molliq.2017.03.036.
[17] J.M.M. Araújo, A.B. Pereiro, F. Alves, I.M. Marrucho, L.P.N. Rebelo, Nucleic acid bases in 1-alkyl-3-methylimidazolium acetate ionic liquids: A thermophysical and ionic conductivity analysis, J. Chem. Thermodyn. 57 (2013) 1–8, https://doi.org/10.1016/j.jct.2012.07.022.
[18] C.M.S.S. Neves, K.A. Kurnia, J.A.P. Coutinho, I.M. Marrucho, J.N.C. Lopes, M.G. Freire, L.P.N. Rebelo, Systematic Study of the Thermophysical Properties of Imidazolium-Based Ionic Liquids with Cyano-Functionalized Anions, J. Phys. Chem. B 117 (35) (2013) 10271–10283, https://doi.org/10.1021/jp405913b.
[19] J.O. Valderrama, W.W. Sanga, J.A. Lazzús, Critical Properties, Normal Boiling Temperature, and Acentric Factor of Another 200 Ionic Liquids, Ind. Eng. Chem. Res. 47 (4) (2008) 1318–1330, https://doi.org/10.1021/ie071055d.
[20] H.-H. Chen, M.-K. Chen, B.-C. Chen, I.-L. Chien, Critical Assessment of Using an Ionic Liquid as Entrainer via Extractive Distillation, Ind. Eng. Chem. Res. 56 (27) (2017) 7768–7782, https://doi.org/10.1021/acs.iecr.7b01223.
[21] J. Rudkin, Equation Predicts Vapor Pressures, Chem. Eng.: April 17th (1961) 202–203.
[22] C. Su, X. Liu, C. Zhu, M. He, Isobaric molar heat capacities of 1-ethyl-3-methylimidazolium acetate and 1-hexyl-3-methylimidazolium acetate up to 16 MPa, Fluid Phase Equilibr. 427 (2016) 187–193, https://doi.org/10.1016/j.fluid.2016.06.054.
[23] E. Zorębski, M. Musiał, K. Bałuszyńska, M. Zorębski, M. Dzida, Isobaric and Isochoric Heat Capacities as Well as Isentropic and Isothermal Compressibilities of Di- and Trisubstituted Imidazolium-Based Ionic Liquids as a Function of Temperature, Ind. Eng. Chem. Res. 57 (14) (2018) 5161–5172, https://doi.org/10.1021/acs.iecr.8b00506.
[24] H. Renon, J.M. Prausnitz, Local Compositions in Thermodynamic Excess Functions for Liquid Mixtures, AIChE J. 14 (1) (1968) 135–144, https://doi.org/10.1002/aic.690140124.
[25] M.C. Castro, A. Arce, A. Soto, H. Rodríguez, Liquid-liquid equilibria of mutually immiscible ionic liquids with a common anion of basic character, J. Chem. Thermodyn. 102 (2016) 12–21, https://doi.org/10.1016/j.jct.2016.05.023.
[26] M.P. Cumplido, E. Lladosa, S. Loras, J. Pla-Franco, Isobaric vapor-liquid equilibria for extractive distillation of 1-propanol + water mixture using thiocyanate-based ionic liquids, J. Chem. Thermodyn. 113 (2017) 219–228, https://doi.org/10.1016/j.jct.2017.06.014.
[27] E. Quijada-Maldonado, S. van der Boogaart, J.H. Lijbers, G.W. Meindersma, A.B. de Haan, Experimental densities, dynamic viscosities and surface tensions of the ionic liquids series 1-ethyl-3-methylimidazolium acetate and dicyanamide and their binary and ternary mixtures with water and ethanol at T = (298.15 to 343.15 K), J. Chem. Thermodyn. 51 (2012) 51–58, https://doi.org/10.1016/j.jct.2012.02.027.
[28] R. Anantharaj, T. Banerjee, Phase behavior of catalytic deactivated compounds and water with 1-ethyl-3-methylimidazolium acetate [EMIM][OAc] ionic liquid at T = 298.15–323.15 K and p = 1 bar, J. Ind. Eng. Chem. 18 (1) (2012) 331–343, https://doi.org/10.1016/j.jiec.2011.11.096.
[29] Y. Chen, Y. Cao, X. Sun, T. Mu, Hydrogen bonding interaction between acetate-based ionic liquid 1-ethyl-3-methylimidazolium acetate and common solvents, J. Mol. Liq. 190 (2014) 151–158, https://doi.org/10.1016/j.molliq.2013.11.010.
[30] O. Redlich, A.T. Kister, Thermodynamics of Nonelectrolyte Solutions. Algebraic Representation of Thermodynamic Properties and the Classification of Solutions, Ind. Eng. Chem. 40 (2) (1948) 345–348, https://doi.org/10.1021/ie50458a036.
[31] I.M. Smallwood, Handbook of Organic Solvent Properties, Butterworth-Heinemann, London (UK), 1996.